BMC Nephrology

RESEARCH

Open Access

Identification of key necroptosis-related genes and immune landscape in patients with immunoglobulin A nephropathy

Ruikun Hu[1†], Ziyu Liu[2†], Huihui Hou[2†], Jingyu Li[3], Ming Yang[5], Panfeng Feng[4*], Xiaorong Wang[1*] and Dechao Xu[2*]

Abstract

Background Immunoglobulin A nephropathy (IgAN) is a major cause of chronic kidney disease (CKD) and kidney failure. Necroptosis is a novel type of programmed cell death that has been proved to be associated with the pathogenesis of infectious disease, cardiovascular disease, neurological disorders and so on. However, the role of necroptosis in IgAN remains unclear.

Methods In this study, we explored the role of necroptosis-related genes in the pathogenesis of IgAN using a comprehensive bioinformatics method. Microarray datasets GSE93798 and GSE115857 were downloaded from Gene Expression Omnibus (GEO). "limma" package of R software was employed to identify necroptosis-related differentially expressed genes (NRDEGs) between IgAN and healthy controls. GO and KEGG functional enrichment analysis was performed by Clusterprofiler. Least absolute shrinkage and selection operator (LASSO) regression analysis identified hub NRDEGs. We further established a diagnostic model consisting of 7 diagnostic hub NRDEGs and validated the efficacy by an external dataset. The expression of hub genes was confirmed in sc-RNA dataset GSE171314. Immune infiltration, gene set enrichment analysis and transcription factor binding motifs enrichment analysis were conducted to further uncover their roles.

Results 1076 differentially expressed genes were identified between healthy individuals and IgAN patients from RNA-seq dataset GSE9379. Then we cross-linked them with necroptosis-related genes to obtain 9 NRDEGs. LASSO regression analysis screened out 7 hub genes (JUN, CD274, SERTAD1, NFKBIA, H19, UCHL1 and EZH2) of IgAN. We further conducted functional enrichment analysis and constructed the diagnostic model based on dataset GSE93798. GSE115857 was used as the independent validation cohort and indicated a great predictive efficacy. Immune infiltration, gene set enrichment analysis and transcription factor binding motifs enrichment analysis revealed their potential function. Finally, we screened out four drugs that were predicted to have therapeutic value of IgAN.

†Ruikun Hu, Ziyu Liu and Huihui Hou contributed equally to this work.

*Correspondence:
Panfeng Feng
fpf929083891@163.com
Xiaorong Wang
xr0104@ntu.edu.cn
Dechao Xu
xudechao08@163.com
Full list of author information is available at the end of the article

Conclusions In summary, we identified 7 hub necroptosis-associated genes, which can be used as potential genetic biomarkers for IgAN prediction and treatment. Four drugs were predicted as the potential therapeutic solutions. Collectively, we provided insights into the necroptosis-related mechanisms and treatment of IgAN at the transcriptome level.

Keywords Immunoglobulin a nephropathy, Necroptosis, Bioinformatic analysis

Introduction

IgAN is the most prevalent glomerulonephritis globally, characterized by abnormal immunoglobulin A (IgA) accumulations in kidneys accompanied by a mesangial proliferative glomerulonephritis [1. 30%~40% of IgAN patients progress slowly to end-stage renal failure [2]. IgAN impairs the function of filtering in the kidney, leading to hematuria and proteinuria. The confirmed diagnosis is typically achieved through the collection of renal biopsy specimens and subsequent detection of IgA1 using immunofluorescent staining. Current therapy interventions mainly focus on supportive treatments as blood pressure control, proteinuria reduction and high-dose corticosteroid [3, 4], but optional individualized cures are limited. At present, the most common methods to predict and diagnose IgAN are histologic features and relevant parameters such as eGFR, BP, proteinuria, age, ethnicity [5]. The mechanism of IgAN remains elusive since the genetic landscape of IgAN is complex. Significant variations in symptoms and histological alterations are observed in various ethnic populations [6]. Therefore, it is imperative to explore new possible pathogenic mechanisms of IgAN and identify potential therapeutic targets.

Necroptosis is a newly discovered pathway of regulated cell death, morphologically characterized by the loss of plasma membrane integrity, leakage of intracellular contents and organelle swelling [7]. The process of necroptosis is triggered by immune ligands such as Fas, TNF and LPS [8]. The initiation of necroptosis requires the formation of necrosome, a complex consisting of receptor-interacting proteins 1(RIPK1), receptor-interacting proteins 3(RIPK3) and mixed-lineage kinase domain–like pseudokinase(MLKL) [9]. As a highly pro-inflammatory mode of cell death, necroptosis causes the release of DAMPs into the extracellular space, promotes inflammation and activate an immune response [10]. Necroptosis has been reported to be involved in the development of several diseases in multiple organs, including myocardial injury, inflammatory neurodegenerative disease and cancer [11, 12]. Recent studies suggested that necroptosis contributes to acute tubular damage, ischemic reperfusion injury and renal tubulointerstitial fibrosis [13]. However, whether necroptosis takes a part in IgAN needs further research.

By far, no studies have investigated whether necroptosis is associated with the pathogenesis and development of IgAN. In this study, we identified differentially expressed necroptosis-related genes that may play a role in IgAN using datasets downloaded from GEO, then selected 7 signature genes to construct a diagnostic model. We then screened out several potential therapeutic drugs.

Methods

The workflow of this study was demonstrated in Fig. 1. This study is a bioinformatics analysis and does not involve clinical trial registration.

Data collection

Three microarray datasets of IgAN (GSE93798, GSE115857, GSE171314) were downloaded from the GEO database. GSE93798 contains glomerular compartment from 22 healthy individuals and 20 IgAN patients. GSE115857 contains renal biopsies from 7 healthy individuals and 55 IgAN patients. GSE171314 contains Single-cell RNA sequencing (scRNA-seq) information of kidney biopsies from 1 control subjects and 4 IgAN patients. Age, sex, and other clinical covariates were not available for control in their study.

Differentially expressed genes identification

The "limma" package [14] of R software was used to identify differentially expressed genes between IgAN patients and normal controls with the following criteria: *P*.Value < 0.05 and |log2FC| > 0.585. Then, we generated volcano and heat maps for differential gene analysis. Then we crossed them with necroptosis-related genes from GeneCards.

Functional enrichment analysis

Gene Ontology (GO) [15] and Kyoto Encyclopedia of Genes and Genomes (KEGG) [16] enrichment analysis were conducted by "ClusterProfiler"package [17] in R software. A gene set at $p < 0.05$ and $q < 0.05$ was regarded as significantly enriched.

Development of the diagnostic model of necroptosis-related genes

Differentially expressed necroptosis-related genes was selected and LASSO regression was used to construct the diagnostic model. After incorporating the

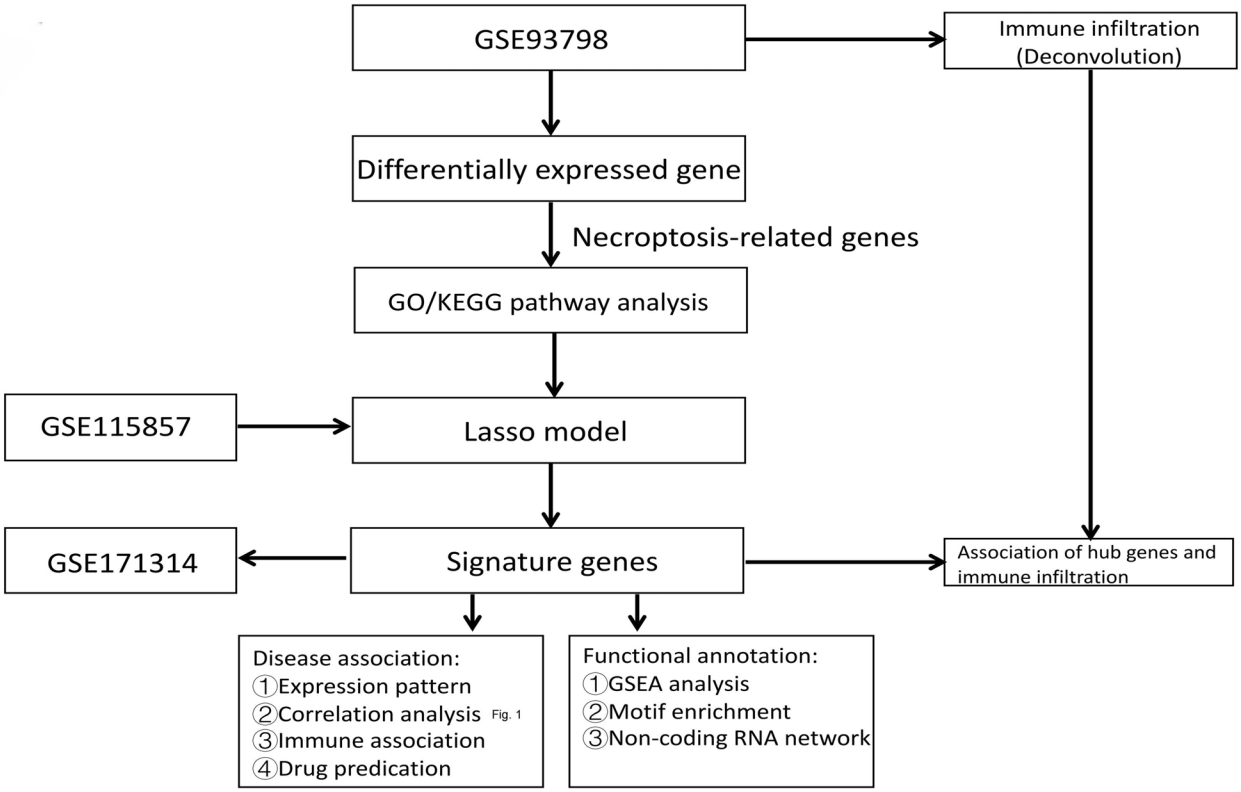

Fig. 1 The workflow of this study

expression values of each gene (denoted by x) and the estimated regression coefficients from the LASSO regression analysis (denoted by β), a risk score was calculated for each patient using the formula: Risk Score = β1·x1 + β2·x2+⋯+βp·xp. A The score for each patient was calculated based on the risk score formula. ROC curves were used to investigate the efficacy and reliability of model.

scRNA-seq data processing

Seurat R package [18] was used for downstream principal component analysis and t-distributed stochastic neighbor embedding (tSNE). The clusters were annotated by the celldex package (https://bioconductor.org/packages/release/data/experiment/vignettes/.

celldex/inst/doc/userguide.html). Marker genes for each cell sub-type from the single cell expression profile were selected by setting the parameter as P.Value adj < 0.05 (calculated using the Benjamini-Hochberg procedure)and |avg log2FC| >1.

Evaluation of immune cell infiltration

The abundance of immune cells in the environment was calculated by CIBERSORT [19]. We used CIBERSORT-based deconvolution combined with LM22 to measure the relative proportion of 22 types of immune subpopulations in GSE93798 and perform spearman correlation analysis of gene expression and immune cell subtypes.

Gene set enrichment analysis (GSEA)

DEGs were divided into two groups (high expression vs. low expression) based on the expression level (median expression) of 7 hub genes. GSEA was exploited to discover the enrichment terms to recognize potential pathways related to IgAN. Text was trimmed and organized using Java script.

Transcription factor binding motifs enrichment analysis

Transcription factor binding motifs (TFBMs) enrichment analysis was performed by The Bioconductor package RcisTarget [20]. The calculation was conducted based on motifs and enrichment score (NES) was normalized to the total number of motifs in the database. We further annotated files based on motif similarity and gene sequences. Firstly, to estimate the overexpression of each motif on a gene set, we calculated the area under the curve (AUC) for each motif-motif pair based on the recovery curve calculation of the gene set to motif ordering. The NES of each motif was calculated based on the AUC distribution of all motifs in the gene set.

Potential therapeutic drug prediction

The Connectivity Map (CMap) [21] is a gene expression profiling databased developed by the Broad Institute. It is used to reveal functional associations between small-molecule compounds, genes and disease states. It contains gene expression profiles of 1.5 million genes from 5,000 small-molecule compounds, and 3,000 genetic reagents, tested in multiple cell types, concentrations and treatment durations. This study used CMap to predict therapeutic agents through differentially expressed genes in IgAN.

Statistical analysis

Statistical analysis was conducted by R software (version 4.2.2) and P.Value < 0.05 was regarded as statistically significant.

Results

Identification of differentially expressed necroptosis-related genes in IgAN

Datasets GSE93798 was downloaded from the NCBI GEO database, including 22 healthy controls and 20 IgAN patients. The differently expressed genes were obtained by limma package with *P*.Value < 0.05 & |log2FC|>0.585. A total of 1076 differentially expressed genes were obtained, including 478 up-regulated genes and 598 down-regulated genes, as shown in Fig. 2a and b and Table S1. Subsequently, necroptosis-related genes with Relevance score > 1 were extracted from GeneCards database and intersected with the DEGs to obtain 9 necroptosis-related differentially expressed genes (NRDEGs), visualized using a Venn diagram (Fig. 2c). The relevance score is calculated by the GeneCards database and is based on term frequency/inverse document frequency (additional details on the scoring can be found here: https://www.genecards.org/Guide/Search#relevance).

GO and KEGG Enrichment analyses

GO analysis revealed that NRDEGs were enriched in cellular response to reactive oxygen species, response to reactive oxygen species and cellular response to oxidative stress (Fig. 3a). The KEGG results indicated that NRDEGs were mainly enriched in IL − 17 signaling pathway, TNF signaling pathway and NOD − like receptor signaling pathway (Fig. 3b).

Construction and validation of a diagnosis-associated risk model

To screen diagnostic signature genes in IgAN, LASSO regression analysis was applied based on the 9 overlapping

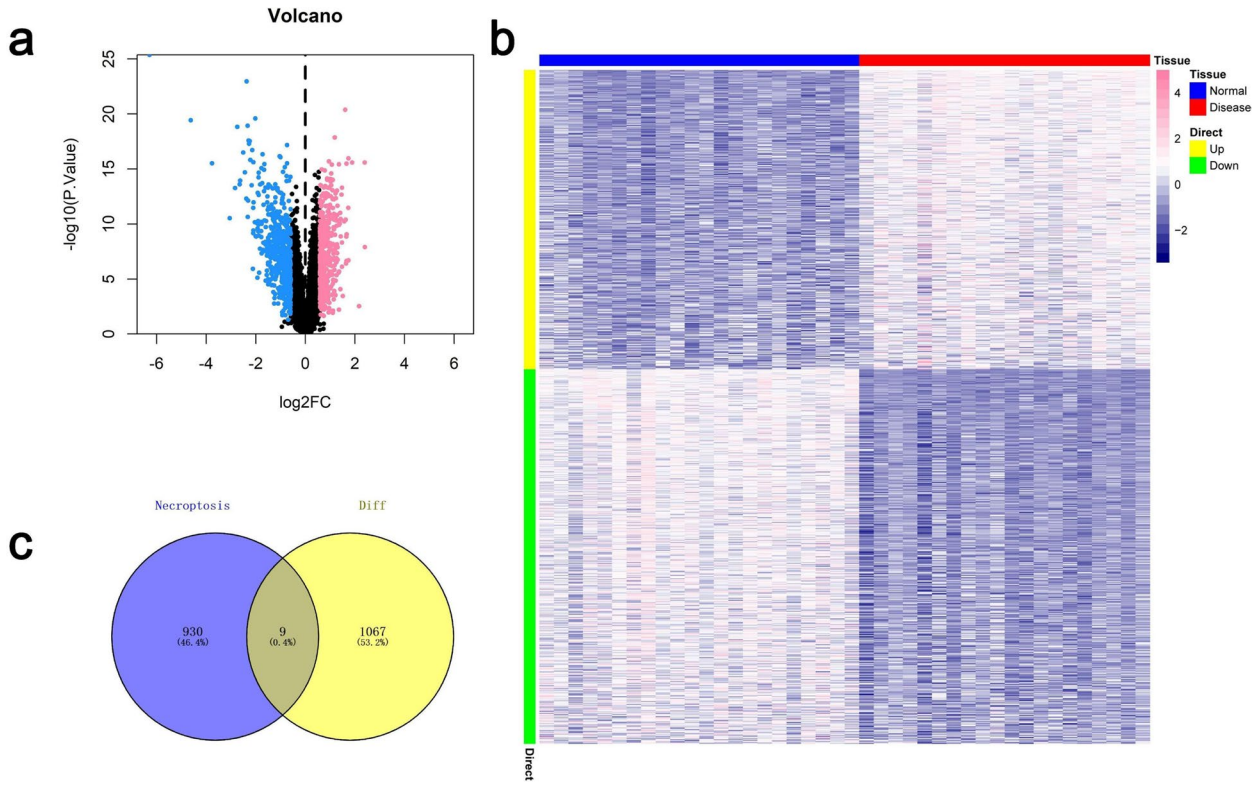

Fig. 2 Identification of DEGs. **a** A volcano plot showing 1076 DEGs in the dataset GSE93798. **b** The heatmap of DEGs. **c** 9 necroptosis-related differentially expressed genes (NRDEGs) were identified after intersection

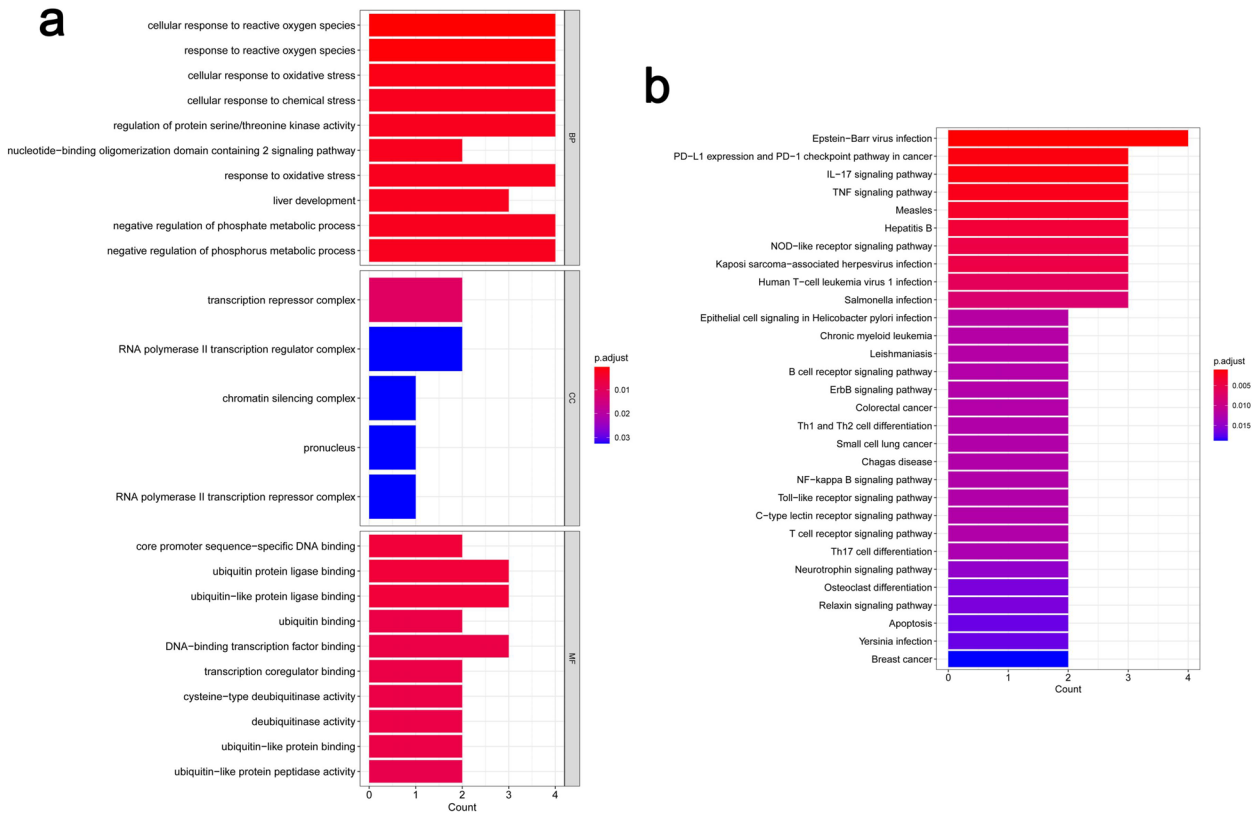

Fig. 3 GO and KEGG enrichment analyses of NRDEGs. **a** GO enrichment of NRDEGs with bar-plot. **b** KEGG analyses of NRDEGs

genes (Fig. 4a, b). LASSO regression analysis identified 7 genes as the characteristic genes for IgAN: JUN, CD274, SERTAD1, NFKBIA, H19, UCHL1 and EZH2 (Fig. 4c, Table S2). We used these 7 genes as hub genes for follow-up study and constructed a diagnostic model. The risk scores for this model were calculated by the following formula: RiskScore = JUN x (−0.23407192090164) + CD274x (−0.0971426727949052) + SERTAD1x (−0.064383446338459) + NFKBIA x (−0.006251764485 15286) + H19 × 0.0213606147376945 + UCHL1 × 0.0780 96134570401 + EZH2 × 0.0943353752022954. As Fig. 4d showed, the area under the curve (AUC) reached 1, indicating the great predictive efficacy of the diagnostic signature in IgAN patients. To verify the stability and reliability of the diagnostic model, GSE115857 dataset from GEO was applied as the external validation. The area under the curve (AUC) was 0.966 (Fig. 4e), demonstrating the great predictive performance of the diagnosis-associated risk model.

Expression of NRDEGs in IgAN at cellular level

To explore the expression of the NRDEGs at single-cell level, we downloaded a sc-RNA (single-cell RNA) dataset GSE171314 from GEO and analyzed by Seurat. Cells were clustered by tSNE and annotated by SingleR [22]. Based on cell features, cells are assigned into Dendritic cells, Monocytes and Progenitors (Fig. 5a, Fig. S1). Figure 5b, c showed the expression level of JUN, CD274, SERTAD1, NFKBIA, H19, UCHL1 and EZH2 in each cell type.

Immune cell infiltration analysis

Microenvironment is composed of immune cells, extracellular matrix, growth factors as well as inflammatory factors, impacting the sensitivity of clinical diagnosis and treatment. To explore the underlying role of NRDEGs in IgAN, we analyzed the differential gene immune infiltration. Figure 6a, b demonstrated the composition of immune cells in each sample and the correlation between each type of immune cell. Compared to healthy controls, the proportion of NK cells activated, macrophages M1, dendritic cells resting, mast cells activated were significantly higher in IgAN patients (Fig. 6c). Moreover, several NRDEGs highly corelated to immune cells (Fig. 6d).

The association between necroptosis-related DEGs and immune-characteristic molecules were analyzed via the TISIDB databases [23]. Figure 7a-e showed the high correlation between NRDEGs and immune and molecular subtypes.

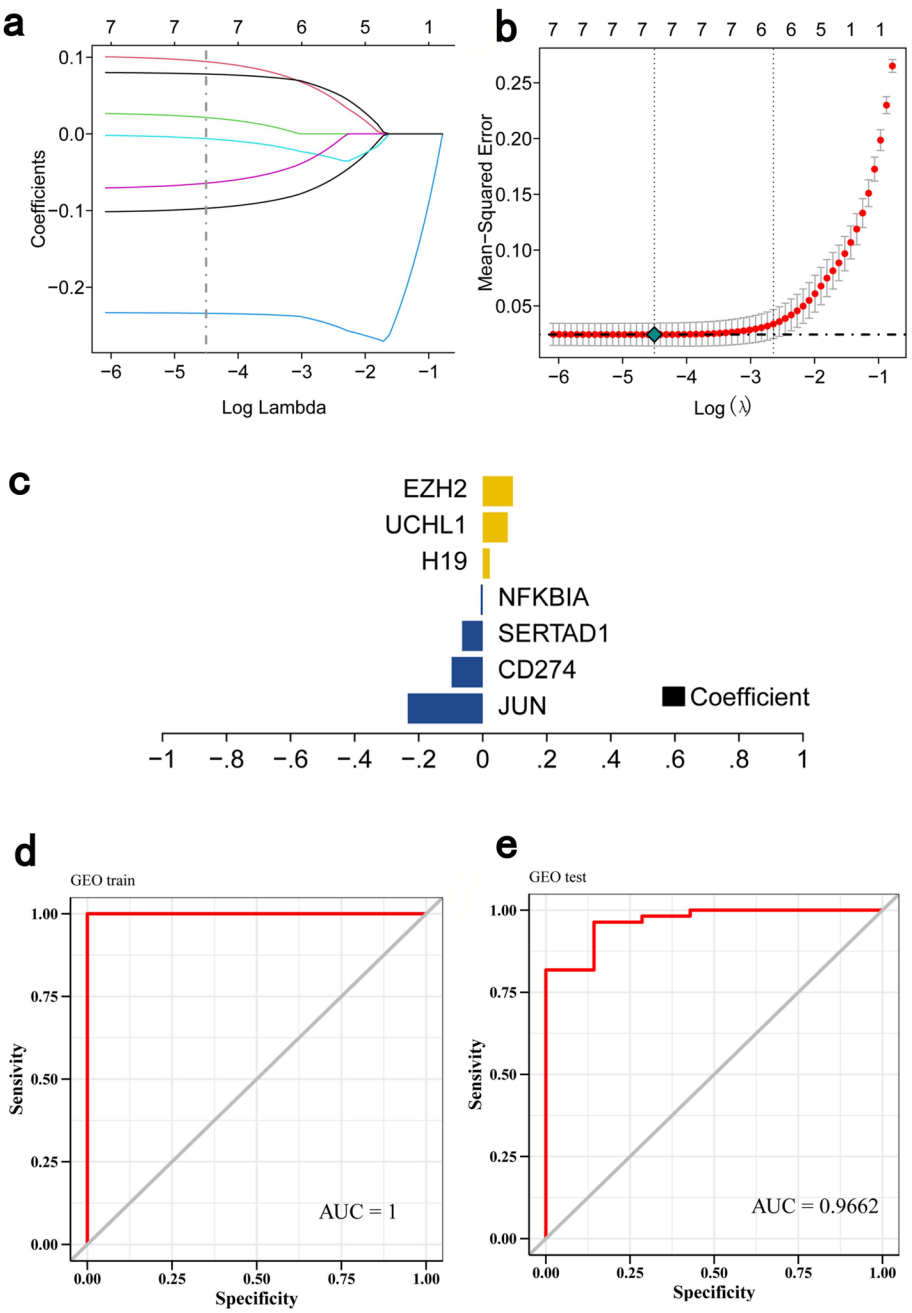

Fig. 4 LASSO regression analysis. **a** LASSO regression identified 7 diagnosis-related genes. **b** The optimal parameter (λ) in the LASSO model. **c** coefficient profiles of the 7 diagnosis-related genes. **d** ROC curves analysis of train set (GSE93798) **e** ROC curves analysis of validation set (GSE115857)

Gene set enrichment analysis

GSEA (gene set enrichment analysis) was then employed to explore the functional roles of NRDEGs. CD274 was enriched in pathways such as aminoacyl tRNA-biosynthesis and insulin signaling. EZH2IS was enriched in pathways such as cell cycle and lysine degradation. H19 was enriched in pathways such as Fc epsilon RI signaling and homologous recombination. JUN was enriched in pathways such as ErbB signaling and histidine metabolism. NFKBIA was enriched in ErbB signaling pathway and histidine metabolism. SERTAD1 was enriched in pathways such as arginine and proline metabolism and adipocytokine signaling pathway. UCH1was enriched in pathways such as ECM (extracellular matrix) receptor interaction and nitrogen metabolism (Fig. 8).

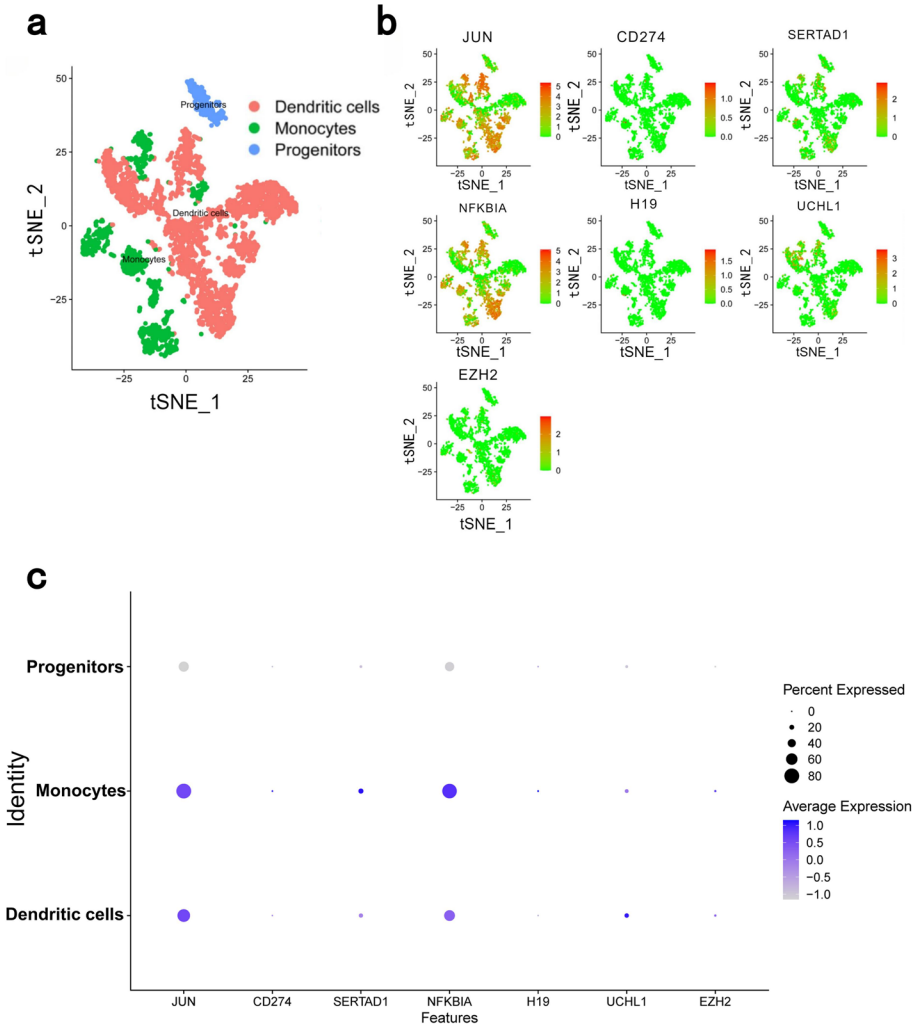

Fig. 5 scRNA analysis of hub genes. **a** Two-dimensional plot from unsupervised clustering by t-distributed stochastic neighbor embedding (tSNE) of the single-cell transcriptomes. Color coded based on cell types. **b** Illustration of the distribution of hub genes in each cell type

Enrichment analysis for transcription factors

We used these 7 hub genes for transcription factor (TF) binding motif enrichment analysis and found that they were regulated by multiple common transcription factors. Cumulative recovery curves were used to enrich these transcription factors. Results showed that the motif with the highest normalized enrichment score (NES:6.19) was cisbp_M5081. Figure 8 demonstrates all enriched motifs and transcription factors (Fig. 9).

The study of IgAN gene expression levels

To explore the change of gene expression levels in patients, 1840 IgAN-related genes were obtained from GeneCards. The expression of ACE, AGT, ALB, CD40LG, COL4A1, COL4A4, COL4A5, PIGR, SPRY2 and TGFB1 was significantly different between healthy controls and patients (Fig. 10a). In addition, expression of the 7 hub genes remarkably correlated with genes related to IgAN. Among which, the expression of JUN negatively correlated to COL4A1 (Pearson r=−0.724) and the expression of SERTAD1 positively correlated to SPRY2 (Pearson r=0.83) (Fig. 10b). We then screened the miRcode database for the 7 hub genes and obtained 76 miRNA and 166 interactive RNA pairs (Fig. 11, Table S3).

Potential drug candidates of NRDEGs Profile

The Connectivity Map (cMap) analysis was performed to identify possible drugs for IgAN using hub genes. DEGs were divided into upregulated and downregulated groups. Top100 genes in each group were uploaded to the CMAP database. Results showed that

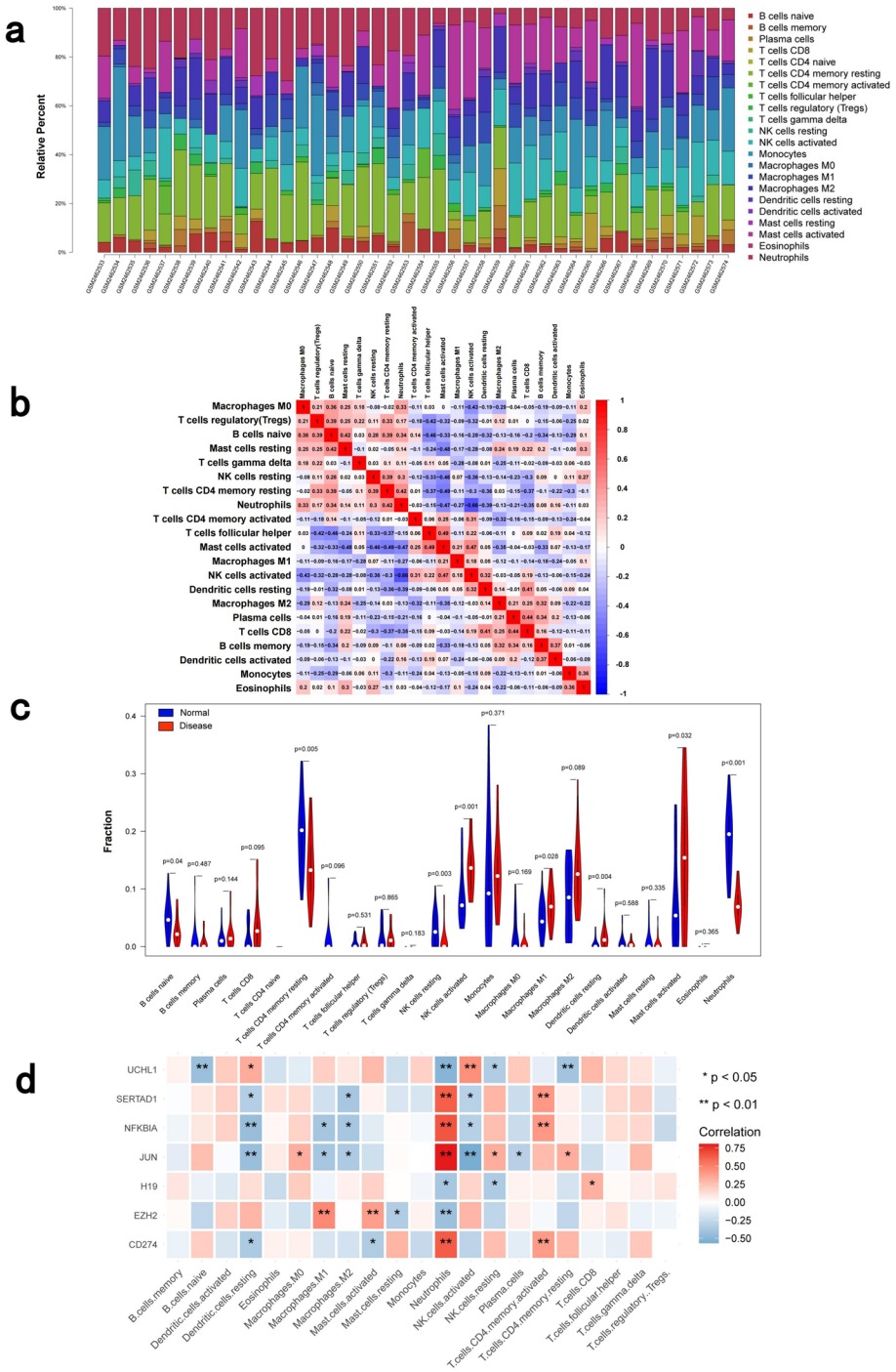

Fig. 6 The landscape of immune infiltration in IgAN. **a** Relative proportion of 22 types of immune cells in IgAN. **b** Heatmap of the correlation between immune cells. **c** The violin plot revealed the immune cell expressions were different in two groups. **d** Correlation analysis between NRDEGs and immune cells

Tyrphostin_AG_126 (ERK1 and ERK2 phosphorylation inhibitor), Verrucarin_A (Protein synthesis inhibitor), Cephaeline (Protein synthesis inhibitor) and Homoharringtonine (Protein synthesis inhibitor) may be able to alleviate or reverse the disease states of IgAN (Fig. 12).

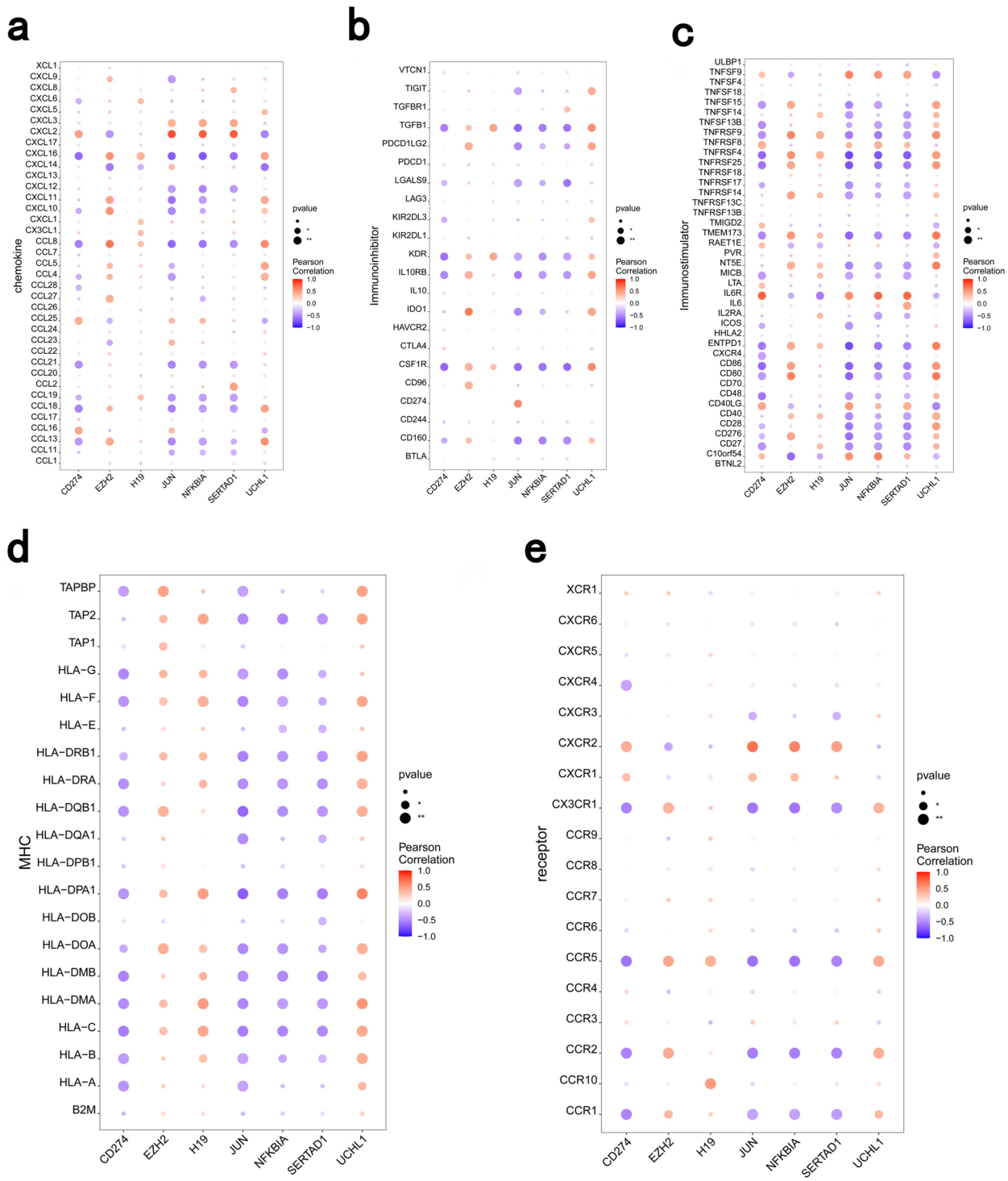

Fig. 7 Analysis of immune infiltration in TISIDB

Discussion

Traditionally, cell death can be categorized into two types: necrotic cell death and programmed cell death depending on whether the process is predefined. In recent years, other forms of cell death have been discovered, including necroptosis, ferroptosis, cuproptosis, oncosis and pyroptosis [24]. Necroptosis, as a highly regulated necrotic death, is mediated by RIPK1-RIPK3-MLKL cascade. Necroptosis

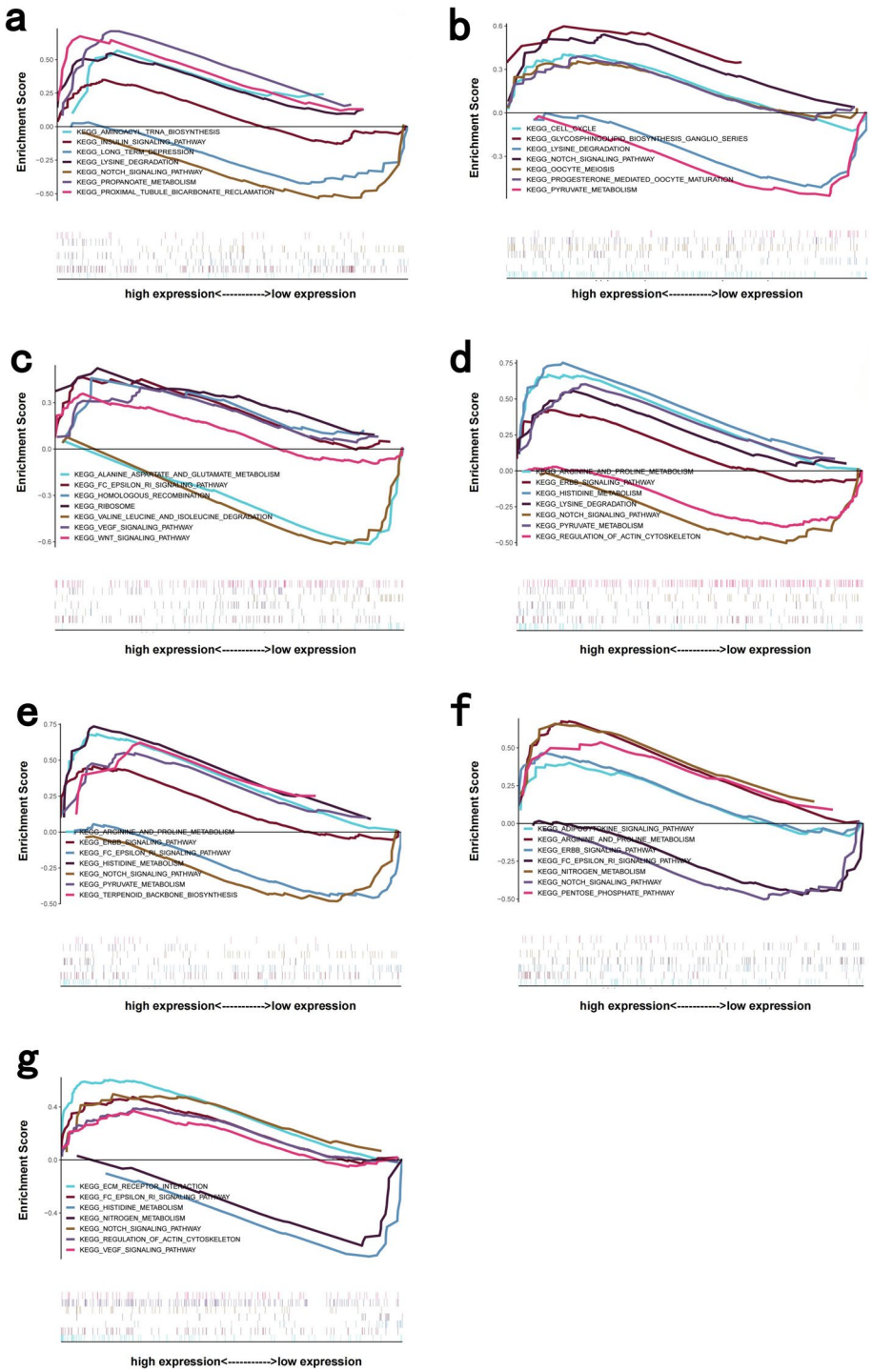

Fig. 8 Gene set enrichment analysis (GSEA) of hub genes

participates in multiple diseases, including atherosclerosis cardiovascular disease, acute respiratory distress syndrome, liver injury, ocular disease, cancers and so on [25, 26]. In kidney disease, essential proteins of necroptosis such as RIPK1, RIPK3, MLKL and repulsive guidance molecules-b(RGM) contribute to AKI [27]. In the model of in the sepsis-induced acute kidney injury, blockade of RIPK1 and RIPK3 prevent kidney tubular injury [28, 29]. In patients with advanced CKD, necrotic renal tubular epithelia cells, as well as the expression level of RIP3 and MLKL, were significantly

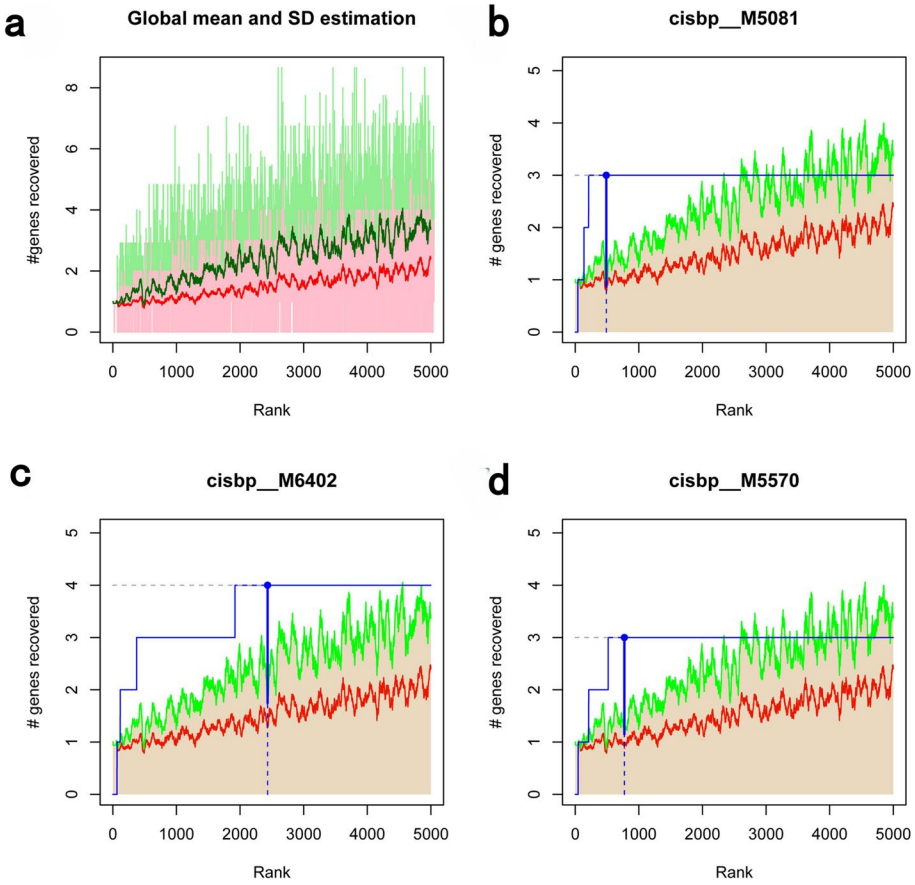

Fig. 9 The enrichment analysis of transcription factors of hub genes

higher [30]. In the development of IgAN, necroptosis may play an important role. On one hand, mesangial cells are under pressure of inflammatory mediator, oxidative stress and cytokines, which is likely to cause necroptosis [31]. On the other hand, pathologic changes during IgAN progression may lead to necroptosis of mesangial cells [32].

This work identified the signature genes of necroptosis that were related to IgAN by analyzing the DEGs between IgAN patients and healthy individuals. 9 NRDEGs were obtained by cross-linking GSE93798 with necroptosis-related genes from GeneCards. Then, we performed GO and KEGG functional enrichment analysis to explore the GO terms and pathways that enriched of the NRDEGs. The response to oxidative stress and cellular response to reactive oxygen species were significantly enriched in the NRDEGs, indicating that NRDEGs were associated with oxidative stress, in line with former research which suggested oxidative stress correlated with serum Gd-IgA1 levels [33]. Previous studies revealed that oxidative stress may regulate the nephrotoxicity of aberrantly glycosylated IgA1 in IgAN [34]. Reactive oxygen species (ROS)are required for BV6/TNFα-induced necroptotic signaling and regulate it by stabilizing necrosome [35]. KEGG pathway analysis revealed that NRDEGs were mostly enriched in Epstein-Barr virus infection. The involvement of Epstein-Barr virus infection in IgAN has been reported in several studies [36]. In African American IgAN patients, enrichment of IgA-expressing B cells infected with Epstein-Barr virus (EBV) was observed, causing the production of galactose-deficient IgA1 [37].

We then performed LASSO regression analysis and identified 7 hub necroptosis-related genes (JUN, CD274, SERTAD1, NFKBIA, H19, UCHL1 and EZH2) and suggest their potential roles in IgAN. JUN is a key component of the transcription factor complex AP-1, regulating cell proliferation and stress response [38]. Research on the role of JUN in kidney diseases mainly focus on cystic kidney. During the progression of human acquired cystic kidney disease (ACKD), the activation of c-Jun is observed in glomerular and tubular cells [39]. In mouse PKD model, inhibition of *Jnk1* and *Jnk2* impair the nuclear accumulation of phospho c-Jun, thus decreasing proliferation and ameliorate the severity [40]. How JUN is related to IgAN needs more investigation. Drugs targeting CD274(PD-L1) has

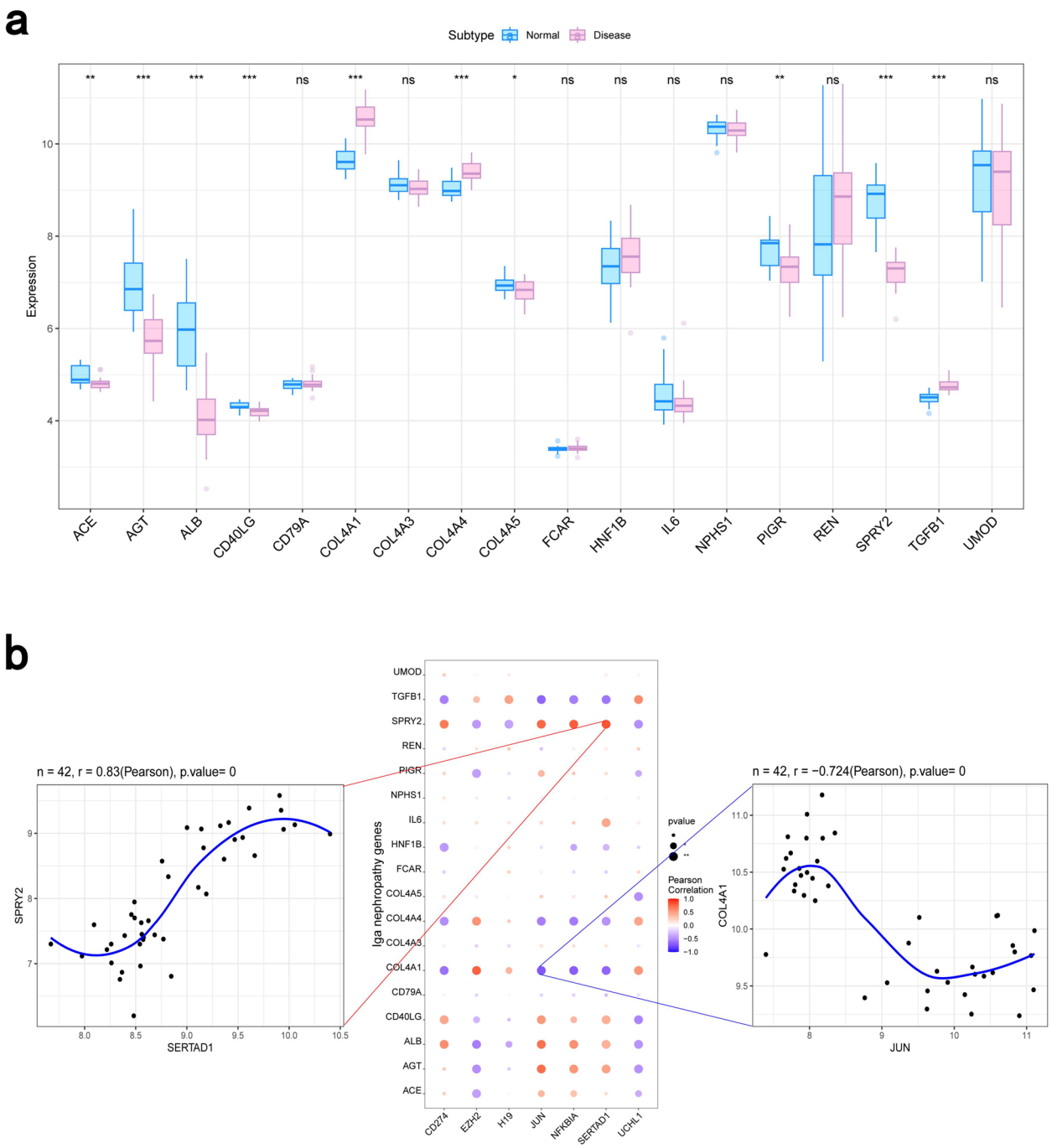

Fig. 10 The relationship of hub genes and the IgAN-related genes. The comparisons of the expression of multiple disease-related genes between the healthy and IgAN patients. (b) Bubble map for the pearson correlations between seven hub genes and IgAN-related

been applied to the treatment of kidney cancers including glomerulonephritis and metastatic renal cell carcinoma [41, 42]. Upregulation of PD-1 signaling is observed in focal segmental glomerulosclerosis in mouse model [43]. Our studies suggest a role of PD-L1 in IgAN but more research is needed to clarify the specific mechanism. SERTAD1 (serine/threonine-rich adaptor protein) is a Cdk4 (cyclin-dependent kinase 4) activator that plays a role in regulating cell growth, proliferation, and differentiation [44]. Differential expression of SERTAD1 was observed in several cancers, including breast cancer, colon cancer, lung cancer, brain tumors and renal cancer [45].

Fig. 11 miRNA-mRNA interaction network

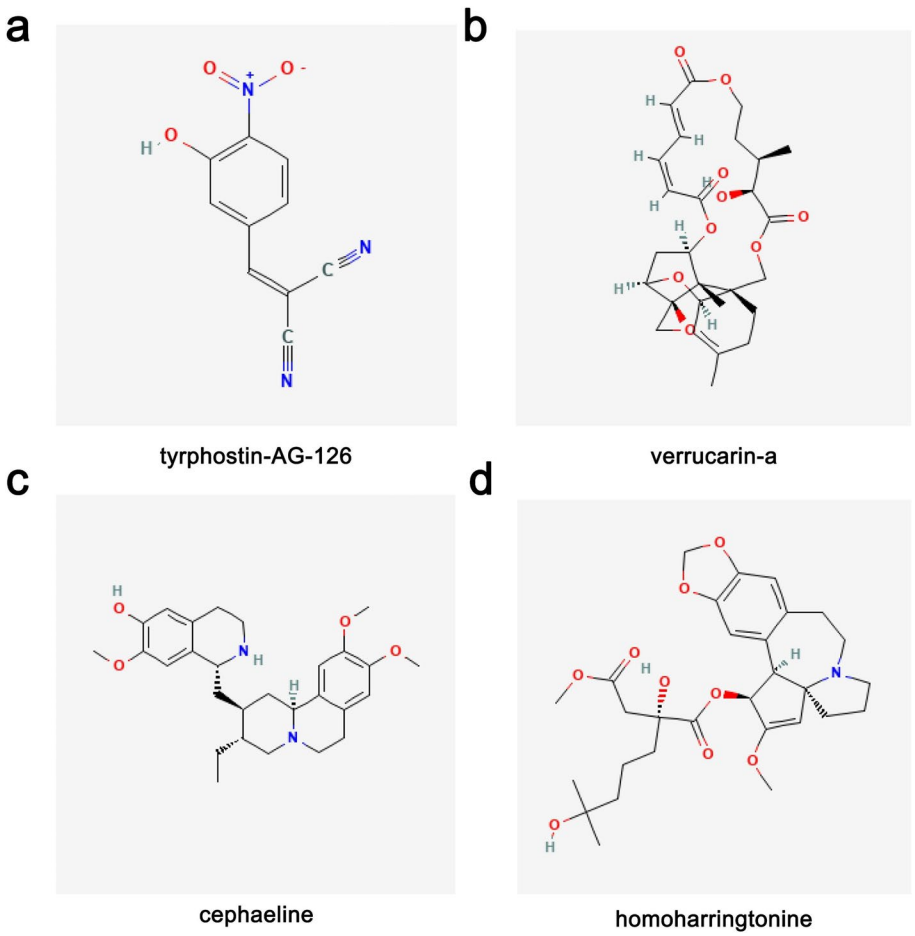

Fig. 12 Potential therapeutic compounds identified by cMap

However, the relation between SERTAD1 and IgAN needs further studies to clarify. NFKBIA is an inhibitor of NF-κB. The relationship between NFKBIA and kidney disease is rarely discussed, but there are studies about its pro-inflammatory role. The expression of NFBIA significantly correlated to the production of inflammatory cytokines [46]. H19 is a long non-coding RNA that participates in oncogenic behaviors in many human cancers [47]. Expression of H19 positively correlated to the development of CaOx nephrocalcinosis-induced oxidative stress and renal tubular epithelial cell injury [48]. H19 has been reported as a potential therapeutic target in many studies. In diabetic mice model, suppression of H19 alleviates kidney fibrosis [49]. Overexpression of H19 significantly improves kidney function in I/R injury mice model [50]. During the transition of AKI to CKD, H19 promotes kidney fibrosis by regulating the miR-196a-5p/Wnt/β-catenin signaling pathway [51]. Little studies focus on the association between UCHL1 and kidney disease, but its role in inflammation has been reported. Knockdown of UCHL1 decreased the number of the key pro-inflammatory cytokines, such as interleukin-6 and tumor necrosis factor-α in macrophages [52].Enhancer of zeste homolog 2 (EZH2) acts as a methyltransferase responsible for inducing histone H3 lysine 27 trimethylation (H3K27me3) and is found to be upregulated in many cancer types [53]. In kidney disease, EZH2 is a potential therapeutic target. EZH2 promotes renal fibrosis by downregulating the expression of Smad7 and PTEN [53]. Inhibition of EZH2 alleviates IR-induced AKI through inactivation of p38 signaling [54]. In cisplatin-induced AKI mouse model, EZH2 inhibition attenuates inflammation by upregulating RKIP and blocking NF-κB p65 signaling [55]. We propose that EZH2 plays a role in IgAN, but the exact mechanism needs further elucidation.

Recent research has described that as the response to innate immune stimuli or genotoxic stress, "RIPoptosome" is assembled and mediates necroptotic signaling [56]. Nevertheless, the underlying mechanism between necroptosis and immunity remains elusive. By investigation the infiltration of immune cells in IgAN, we found that the proportion of NK cells activated, macrophages M1, dendritic cells resting and mast cells activated significantly higher compared to the control group. Macrophages are the predominant inflammatory cells in the renal interstitium [57]. Macrophage M1 facilitate Thl type inflammatory response by secretion of inflammatory factors such as IL-1, IL-6, IL-12 and ROS [58]. The number of macrophages was found increased in IgAN patients. The ability of dendritic cells to induce IgA production in naïve B cells was impaired in IgAN patients [59]. In mouse model, overexpression of indoleamine 2,3-dioxygenase (IDO) on dendritic cells reduced IgAN deposition in glomerular mesangium [60]. Among patients of primary and secondary glomerulonephritis with IgAN, the number of mast cell decreased patients whose renal function rarely deteriorated [61]. Mast cells were distributed in the fibrotic areas in interstitium. The number of mast cells significantly associated with renal functional parameters such as BUN, urinary protein excretion and creatinine clearance, suggesting its role in the progression of interstitial fibrosis [62].

MicroRNAs (miRNA) are reported to be involved in the pathogenesis of IgAN. For example, upregulated microRNA-21-5p (miR-21) leads to the accumulation of IgA1 by inhibiting SPRY1 and inducing Th17 polarization [63]. Several miRNAs serve as non-invasive markers of IgAN diagnosis, including miR-150, miR-204, miR-431 and miR-555 [64–66].

Taken together, this work highlighted the important role of necroptosis in IgAN. However, some limitations still remained in the study. Firstly, no other kidney disease control group was included. There is a possibility that DEGs were not specific to IgAN but generic symptoms like proteinuria. In addition, our conclusion is based on public databases, and it would be a great help to validate our results using clinical samples in the further.

Conclusion

In the study, we identified several necroptosis-related genes that are highly associated with IgAN pathogenesis. A well-validated diagnostic model was established on 7 hub genes and four drugs were screened out as the potential therapeutic molecules. These findings may provide a novel perspective for IgAN clinical diagnosis and treatment.

Abbreviations

IgAN	Immunoglobulin A nephropathy
CKD	C hronic kidney disease
LASSO	Least absolute shrinkage and selection operator
GO	Gene Ontology
KEGG	Kyoto Encyclopedia of Genes and Genomes
AUC	The area under the curve
GSEA	G ene set enrichment analysis

Supplementary Information

The online version contains supplementary material available at https://doi.org/10.1186/s12882-024-03885-4.

Supplementary Material 1: Table S1. The identified 1076 differentially expressed genes.

Supplementary Material 2: Table S2. The exact estimated values of the identified 7 genes.

Supplementary Material 3: Table S3. The interactive RNA pairs.

Supplementary Material 4: Fig. S1. Bubble chart show the cell features used to distinguish cell subsets in the scRNA-seq.

Authors' contributions

Dechao Xu conceived the idea and designed the study. Ming Yang and Xiaorong Wang performed the data analysis. Ruikun hu and Jingyu Li performed the data analysis and wrote the main manuscript. Huihui Hou, Ziyu Liu and Panfeng Feng helped to polish the manuscript.

Funding
This work was supported by the National Natural Science Foundation of China (Grant No.82202063) .

Data availability
The datasets were downloaded from the National Center for Biotechnology Information Gene Expression Omnibus (GEO). GSE93798: https://www.ncbi.nlm.nih.gov/geo/query/acc.cgi?acc=GSE93798. GSE115857: https://www.ncbi.nlm.nih.gov/geo/query/acc.cgi?acc=GSE115857. GSE171314 : https://www.ncbi.nlm.nih.gov/geo/query/acc.cgi?acc=GSE171314.

Declarations

Ethics approval and consent to participate
Not applicable.

Consent for publication
Not applicable.

Competing interests
The authors declare no competing interests.

Author details
[1]Affiliated Maternity and Child Health Care Hospital of Nantong University, Nantong, Jiangsu 226001, China. [2]Department of Nephrology, Changzheng Hospital, Naval Medical University, Shanghai 200003, China. [3]School of Life Sciences and Technology, Tongji University, Shanghai 200092, China. [4]Department of Pharmacy, The First People's Hospital of Nantong city, Affiliated Hospital 2 of Nantong University, Nantong, Jiangsu 226001, China. [5]Department of Nephrology, Shanghai Fourth People's Hospital, School of Medicine, Tongji University, Shanghai 200434, China.

Received: 1 April 2024 Accepted: 25 November 2024
Published online: 18 December 2024

References

1. Moresco RN, Speeckaert MM, Delanghe JR. Diagnosis and monitoring of IgA nephropathy: the role of biomarkers as an alternative to renal biopsy. Autoimmun Rev. 2015;14(10):847–53.
2. Lai KN, Tang SC, Schena FP, Novak J, Tomino Y, Fogo AB, Glassock RJ. IgA nephropathy. Nat Rev Dis Primers. 2016;2:16001.
3. Nagasawa Y, Yamamoto R, Shinzawa M, Shoji T, Hasuike Y, Nagatoya K, Yamauchi A, Hayashi T, Kuragano T, Moriyama T, et al. Efficacy of corticosteroid therapy for IgA nephropathy patients stratified by kidney function and proteinuria. Clin Exp Nephrol. 2020;24(10):927–34.
4. Floege J, Rauen T, Tang SCW. Current treatment of IgA nephropathy. Semin Immunopathol. 2021;43(5):717–28.
5. Aucella F, Netti GS, Piemontese M, Cincione IR, Infante B, Gesualdo L. Proteinuria in the prognosis of IgA nephropathy. Minerva Urol Nefrol. 2009;61(3):235–48.
6. Hall YN, Fuentes EF, Chertow GM, Olson JL. Race/ethnicity and disease severity in IgA nephropathy. BMC Nephrol. 2004;5:10.
7. Vanden Berghe T, Vanlangenakker N, Parthoens E, Deckers W, Devos M, Festjens N, Guerin CJ, Brunk UT, Declercq W, Vandenabeele P. Necroptosis, necrosis and secondary necrosis converge on similar cellular disintegration features. Cell Death Differ. 2010;17(6):922–30.
8. Dhuriya YK, Sharma D. Necroptosis: a regulated inflammatory mode of cell death. J Neuroinflammation. 2018;15(1):199.
9. Chen J, Kos R, Garssen J, Redegeld F. Molecular insights into the mechanism of necroptosis: The necrosome as a potential therapeutic target. Cells. 2019;8(12):1486.
10. Negroni A, Colantoni E, Cucchiara S, Stronati L. Necroptosis in intestinal inflammation and Cancer: New concepts and therapeutic perspectives. Biomolecules. 2020;10(10):1431.
11. Galluzzi L, Kepp O, Chan FK, Kroemer G. Necroptosis: mechanisms and relevance to disease. Annu Rev Pathol. 2017;12:103–30.
12. Chaouhan HS, Vinod C, Mahapatra N, Yu SH, Wang IK, Chen KB, Yu TM, Li CY. Necroptosis: a pathogenic negotiator in human diseases. Int J Mol Sci. 2022;23(21):12714.
13. Jun W, Benjanuwattra J, Chattipakorn SC, Chattipakorn N. Necroptosis in renal ischemia/reperfusion injury: a major mode of cell death? Arch Biochem Biophys. 2020;689:108433.
14. Ritchie ME, Phipson B, Wu D, Hu Y, Law CW, Shi W, Smyth GK. Limma powers differential expression analyses for RNA-sequencing and microarray studies. Nucleic Acids Res. 2015;43(7):e47.
15. Ashburner M, Ball CA, Blake JA, Botstein D, Butler H, Cherry JM, Davis AP, Dolinski K, Dwight SS, Eppig JT, et al. Gene ontology: tool for the unification of biology. The gene ontology consortium. Nat Genet. 2000;25(1):25–9.
16. Kanehisa M, Goto S. KEGG: kyoto encyclopedia of genes and genomes. Nucleic Acids Res. 2000;28(1):27–30.
17. Yu G, Wang LG, Han Y, He QY. clusterProfiler: an R package for comparing biological themes among gene clusters. OMICS. 2012;16(5):284–7.
18. Butler A, Hoffman P, Smibert P, Papalexi E, Satija R. Integrating single-cell transcriptomic data across different conditions, technologies, and species. Nat Biotechnol. 2018;36(5):411–20.
19. Newman AM, Liu CL, Green MR, Gentles AJ, Feng W, Xu Y, Hoang CD, Diehn M, Alizadeh AA. Robust enumeration of cell subsets from tissue expression profiles. Nat Methods. 2015;12(5):453–7.
20. Aibar S, Hulselmans G, Aerts S. RcisTarget: identify transcription factor binding motifs enriched on a gene list. 2022. https://www.bioconductor.org/packages/release/bioc/html/RcisTarget.html.
21. Lamb J, Crawford ED, Peck D, Modell JW, Blat IC, Wrobel MJ, Lerner J, Brunet JP, Subramanian A, Ross KN, et al. The Connectivity Map: using gene-expression signatures to connect small molecules, genes, and disease. Science. 2006;313(5795):1929–35.
22. Aran D, Looney AP, Liu L, Wu E, Fong V, Hsu A, Chak S, Naikawadi RP, Wolters PJ, Abate AR, et al. Reference-based analysis of lung single-cell sequencing reveals a transitional profibrotic macrophage. Nat Immunol. 2019;20(2):163–72.
23. Ru B, Wong CN, Tong Y, Zhong JY, Zhong SSW, Wu WC, Chu KC, Wong CY, Lau CY, Chen I, et al. TISIDB: an integrated repository portal for tumor-immune system interactions. Bioinformatics. 2019;35(20):4200–2.
24. D'Arcy MS. Cell death: a review of the major forms of apoptosis, necrosis and autophagy. Cell Biol Int. 2019;43(6):582–92.
25. Liu Y, Liu T, Lei T, Zhang D, Du S, Girani L, Qi D, Lin C, Tong R, Wang Y. RIP1/RIP3-regulated necroptosis as a target for multifaceted disease therapy (review). Int J Mol Med. 2019;44(3):771–86.
26. Gong Y, Fan Z, Luo G, Yang C, Huang Q, Fan K, Cheng H, Jin K, Ni Q, Yu X, et al. The role of necroptosis in cancer biology and therapy. Mol Cancer. 2019;18(1):100.
27. Anders HJ. Necroptosis in Acute kidney Injury. Nephron. 2018;139(4):342–8.
28. Dong W, Li Z, Chen Y, Zhang L, Ye Z, Liang H, Li R, Xu L, Zhang B, Liu S, et al. Necrostatin-1 attenuates sepsis-associated acute kidney injury by promoting autophagosome elimination in renal tubular epithelial cells. Mol Med Rep. 2018;17(2):3194–9.
29. Sureshbabu A, Patino E, Ma KC, Laursen K, Finkelsztein EJ, Akchurin O, Muthukumar T, Ryter SW, Gudas L, Choi AMK, et al. RIPK3 promotes sepsis-induced acute kidney injury via mitochondrial dysfunction. JCI Insight. 2018;3(11):e98411.
30. Lin Z, Chen A, Cui H, Shang R, Su T, Li X, Wang K, Yang J, Gao K, Lv J, et al. Renal tubular epithelial cell necroptosis promotes tubulointerstitial fibrosis in patients with chronic kidney disease. FASEB J. 2022;36(12):e22625.
31. Rauen T, Floege J. Inflammation in IgA nephropathy. Pediatr Nephrol. 2017;32(12):2215–24.
32. Gomez-Guerrero C, Hernandez-Vargas P, Lopez-Franco O, Ortiz-Munoz G, Egido J. Mesangial cells and glomerular inflammation: from the pathogenesis to novel therapeutic approaches. Curr Drug Targets Inflamm Allergy. 2005;4(3):341–51.
33. Caliskan Y, Demir E, Karatay E, Ozluk Y, Mirioglu S, Dirim AB, Artan AS, Usta Akgul S, Oto OA, Savran Oguz F, et al. Oxidative stress and macrophage infiltration in IgA nephropathy. J Nephrol. 2022;35(4):1101–11.
34. Camilla R, Suzuki H, Dapra V, Loiacono E, Peruzzi L, Amore A, Ghiggeri GM, Mazzucco G, Scolari F, Gharavi AG, et al. Oxidative stress and galactose-deficient IgA1 as markers of progression in IgA nephropathy. Clin J Am Soc Nephrol. 2011;6(8):1903–11.
35. Schenk B, Fulda S. Reactive oxygen species regulate Smac mimetic/TNFalpha-induced necroptotic signaling and cell death. Oncogene. 2015;34(47):5796–806.

36. Mestecky J, Julian BA, Raska M. IgA nephropathy: pleiotropic impact of Epstein-Barr virus infection on immunopathogenesis and racial incidence of the disease. Front Immunol. 2023;14:1085922.
37. Zachova K, Kosztyu P, Zadrazil J, Matousovic K, Vondrak K, Hubacek P, Julian BA, Moldoveanu Z, Novak Z, Kostovcikova K, et al. Role of Epstein-Barr Virus in Pathogenesis and racial distribution of IgA Nephropathy. Front Immunol. 2020;11:267.
38. Meixner A, Karreth F, Kenner L, Penninger JM, Wagner EF. Jun and JunD-dependent functions in cell proliferation and stress response. Cell Death Differ. 2010;17(9):1409–19.
39. Kobayashi A, Takahashi T, Horita S, Yamamoto I, Yamamoto H, Teraoka S, Tanabe K, Hosoya T, Yamaguchi Y. Activation of the transcription factor c-Jun in acute cellular and antibody-mediated rejection after kidney transplantation. Hum Pathol. 2010;41(12):1682–93.
40. Smith AO, Jonassen JA, Preval KM, Davis RJ, Pazour GJ. c-Jun N-terminal kinase (JNK) signaling contributes to cystic burden in polycystic kidney disease. PLoS Genet. 2021;17(12):e1009711.
41. Aggen DH, Drake CG, Rini BI. Targeting PD-1 or PD-L1 in metastatic kidney cancer: combination therapy in the First-Line setting. Clin Cancer Res. 2020;26(9):2087–95.
42. Curran CS, Kopp JB. PD-1 immunobiology in glomerulonephritis and renal cell carcinoma. BMC Nephrol. 2021;22(1):80.
43. Pippin JW, Kaverina N, Wang Y, Eng DG, Zeng Y, Tran U, Loretz CJ, Chang A, Akilesh S, Poudel C, et al. Upregulated PD-1 signaling antagonizes glomerular health in aged kidneys and disease. J Clin Invest. 2022;132(16):e156250.
44. Biswas SC, Zhang Y, Iyirhiaro G, Willett RT, Rodriguez Gonzalez Y, Cregan SP, Slack RS, Park DS, Greene LA. Sertad1 plays an essential role in developmental and pathological neuron death. J Neurosci. 2010;30(11):3973–82.
45. Mongre RK, Jung S, Mishra CB, Lee BS, Kumari S, Lee MS. Prognostic and clinicopathological significance of SERTAD1 in various types of Cancer Risk: a systematic review and retrospective analysis. Cancers (Basel). 2019;11(3):337.
46. Ping Z, Chen S, Hermans SJF, Kenswil KJG, Feyen J, van Dijk C, Bindels EMJ, Mylona AM, Adisty NM, Hoogenboezem RM, et al. Activation of NF-kappaB driven inflammatory programs in mesenchymal elements attenuates hematopoiesis in low-risk myelodysplastic syndromes. Leukemia. 2019;33(2):536–41.
47. Yang J, Qi M, Fei X, Wang X, Wang K. LncRNA H19: a novel oncogene in multiple cancers. Int J Biol Sci. 2021;17(12):3188–208.
48. Liu H, Ye T, Yang X, Liu J, Jiang K, Lu H, Xia D, Peng E, Chen Z, Sun F, et al. H19 promote calcium oxalate nephrocalcinosis-induced renal tubular epithelial cell injury via a ceRNA pathway. EBioMedicine. 2019;50:366–78.
49. Gysel C. Marginal notes on the anatomy of the masticatory system according to Govert Bidloo (1685) and William Cowper (1698). Rev Belge Med Dent (1984). 1987;42(4):125–9.
50. Haddad G, Kolling M, Wegmann UA, Dettling A, Seeger H, Schmitt R, Soerensen-Zender I, Haller H, Kistler AD, Dueck A, et al. Renal AAV2-Mediated overexpression of long non-coding RNA H19 attenuates ischemic acute kidney Injury through sponging of microRNA-30a-5p. J Am Soc Nephrol. 2021;32(2):323–41.
51. Dong X, Cao R, Li Q, Yin L. The long noncoding RNA-H19 mediates the progression of fibrosis from Acute kidney Injury to chronic kidney disease by regulating the miR-196a/Wnt/beta-Catenin signaling. Nephron. 2022;146(2):209–19.
52. Zhang Z, Liu N, Chen X, Zhang F, Kong T, Tang X, Yang Q, Chen W, Xiong X, Chen X. UCHL1 regulates inflammation via MAPK and NF-kappaB pathways in LPS-activated macrophages. Cell Biol Int. 2021;45(10):2107–17.
53. Zhou X, Zang X, Ponnusamy M, Masucci MV, Tolbert E, Gong R, Zhao TC, Liu N, Bayliss G, Dworkin LD, et al. Enhancer of Zeste Homolog 2 inhibition attenuates renal fibrosis by maintaining Smad7 and phosphatase and Tensin Homolog expression. J Am Soc Nephrol. 2016;27(7):2092–108.
54. Liang H, Huang Q, Liao MJ, Xu F, Zhang T, He J, Zhang L, Liu HZ. EZH2 plays a crucial role in ischemia/reperfusion-induced acute kidney injury by regulating p38 signaling. Inflamm Res. 2019;68(4):325–36.
55. Wen L, Tao SH, Guo F, Li LZ, Yang HL, Liang Y, Zhang LD, Ma L, Fu P. Selective EZH2 inhibitor zld1039 alleviates inflammation in cisplatin-induced acute kidney injury partially by enhancing RKIP and suppressing NF-kappaB p65 pathway. Acta Pharmacol Sin. 2022;43(8):2067–80.
56. Lu JV, Chen HC, Walsh CM. Necroptotic signaling in adaptive and innate immunity. Semin Cell Dev Biol. 2014;35:33–9.
57. Yoshimura A, Mori W. Renal tissue mast cells in liver diseases. Int Urol Nephrol. 1991;23(5):511–6.
58. Zhou D, Huang C, Lin Z, Zhan S, Kong L, Fang C, Li J. Macrophage polarization and function with emphasis on the evolving roles of coordinated regulation of cellular signaling pathways. Cell Signal. 2014;26(2):192–7.
59. Eijgenraam JW, Woltman AM, Kamerling SW, Briere F, de Fijter JW, Daha MR, van Kooten C. Dendritic cells of IgA nephropathy patients have an impaired capacity to induce IgA production in naive B cells. Kidney Int. 2005;68(4):1604–12.
60. Liu K, Yang Y, Chen Y, Li S, Gong Y, Liang Y. The therapeutic effect of dendritic cells expressing indoleamine 2,3-dioxygenase (IDO) on an IgA nephropathy mouse model. Int Urol Nephrol. 2020;52(2):399–407.
61. Silva GE, Costa RS, Ravinal RC, dos Reis MA, Dantas M, Coimbra TM. Mast cells, TGF-beta1 and alpha-SMA expression in IgA nephropathy. Dis Markers. 2008;24(3):181–90.
62. Ehara T, Shigematsu H. Contribution of mast cells to the tubulointerstitial lesions in IgA nephritis. Kidney Int. 1998;54(5):1675–83.
63. Xu BY, Meng SJ, Shi SF, Liu LJ, Lv JC, Zhu L, Zhang H. MicroRNA-21-5p participates in IgA nephropathy by driving T helper cell polarization. J Nephrol. 2020;33(3):551–60.
64. Szeto CC, Wang G, Ng JK, Kwan BC, Mac-Moune Lai F, Chow KM, Luk CC, Lai KB, Li PK. Urinary miRNA profile for the diagnosis of IgA nephropathy. BMC Nephrol. 2019;20(1):77.
65. Noor F, Saleem MH, Aslam MF, Ahmad A, Aslam S. Construction of miRNA-mRNA network for the identification of key biological markers and their associated pathways in IgA nephropathy by employing the integrated bioinformatics analysis. Saudi J Biol Sci. 2021;28(9):4938–45.
66. Xu Y, He Y, Hu H, Xu R, Liao Y, Dong X, Song H, Chen X, Chen J. The increased miRNA-150-5p expression of the tonsil tissue in patients with IgA nephropathy may be related to the pathogenesis of disease. Int Immunopharmacol. 2021;100:108124.

Publisher's note